Astigmatism in Gaussian-beam self-focusing and in resonators for Kerr-lens mode locking

V. Magni, G. Cerullo, S. De Silvestri, and A. Monguzzi

Dipartimento di Fisica del Politecnico, Centro di Elettronica Quantistica e Strumentazione Elettronica del Consiglio Nazionale delle Ricerche, Piazza Leonardo da Vinci 32, 20133 Milano, Italy

Received August 8, 1994; revised manuscript received October 20, 1994

An analytical treatment for the propagation of astigmatic Gaussian beams in Kerr media is presented. This method, which is valid to the first order in the beam power, allows us to calculate in closed form the nonlinear variations of the spot size and the radius of curvature. This formalism is applied to the calculation of the self-consistent Gaussian mode of an astigmatic resonator with a Kerr medium, such as those used for Kerr-lens mode-locked lasers. Theoretical predictions are confirmed by the experimental results obtained with a femtosecond Ti:sapphire laser. In particular, the design of an optimized resonator permits self-starting of the mode-locking mechanism.

1. INTRODUCTION

In past years self-focusing effects in materials with fast Kerr nonlinearities have found an important application in laser mode locking for the generation of ultrashort light pulses. In the Kerr-lens mode-locking (KLM) technique the intracavity self-focusing effect, combined with an internal aperture, results in nonlinear power-dependent resonator losses that sustain the mode-locking regime.[1,2] Typically the Kerr nonlinearity acts on beams with a power significantly lower than the critical power for self-trapping, and the transverse profile remains essentially Gaussian.

The propagation of beams with cylindrical symmetry in Kerr media has been studied in depth both analytically and numerically (for a review see Refs. 3–6). For low beam powers the aberrationless approximation,[3,4] according to which the transverse variation of the refractive index is assumed to be parabolic, provides a great mathematical simplification of the problem and yields quite accurate results. Within this context the propagation of a cylindrically symmetric Gaussian beam can be described by simple closed-form equations.[3,7–9] Also, the self-consistent Gaussian mode in a cylindrically symmetric resonator containing a Kerr medium can be easily calculated, and the dependence on the beam power can be expressed in closed form.[9] However, the resonators used in practice for KLM usually exhibit astigmatism, which is generally due to Brewster-cut elements and to concave folding mirrors that are not used at normal incidence. In these cases the propagation of astigmatic Gaussian beams through nonlinear Kerr media must be analyzed. A number of papers on the analysis and design of resonators for KLM were published[2,9–20]; however, astigmatism effects were not fully taken into account. Numerical studies pointed out that astigmatism can produce sizable effects even in the so-called astigmatically compensated resonators.[21] For a thorough understanding of resonators used in KLM lasers an analysis of the modes of an astigmatic resonator containing a Kerr medium is therefore essential. For astigmatic Gaussian beams the aberrationless approximation provides differential equations describing the propagation of the beam spot sizes along transverse directions.[22] The solution of these equations was found analytically in an implicit form,[23,24] which, however is not highly amenable to a direct application. The main features of astigmatic Gaussian beams in Kerr media at various power levels were also studied numerically.[25]

Our purpose in this paper is to derive closed-form equations that describe the self-focusing of astigmatic Gaussian beams and to calculate analytically the self-consistent mode in astigmatic resonators with a Kerr medium inside. The theoretical development is based on the three following assumptions: (i) the aberrationless approximation, which consists in taking into account only parabolic nonlinear transverse variations of the refractive index, so that the beam maintains its Gaussian shape during the propagation; (ii) the low-power approximation, which consists in retaining only terms to the first order in the beam power (normalized to the critical power for self-trapping); and (iii) the assumption of instantaneous response of the nonlinearity, so that steady-state equations can be applied to the mode-locking regime also. These hypotheses do not substantially limit the applicability of the results for KLM, since in practice the beams are Gaussian and the power is lower than the critical power for self-trapping. Moreover, the most important parameter for KLM is just the derivative of the mode spot size with respect to the power calculated at a vanishing beam power, since the value of this parameter establishes whether KLM is possible and when self-starting can be achieved. While the first of the assumptions was used in a number of papers, the second has not yet been fully exploited. On these bases we derive closed-form equations for the beam propagation and for the resonator mode calculation for KLM. The validity of the results is assessed by comparison with numerical simulations and demonstrated by experimental measurements performed on a femtosecond KLM Ti:sapphire laser. Since a suitably large nonlinear spot-

0740-3224/95/030476-10$06.00

size variation can permit the self-starting of KLM[26–29] and result in more reliable operation, examples of applications of the general results to different resonators are presented with the aim of finding configurations optimized for the largest mode variations.

2. PROPAGATION OF AN ASTIGMATIC GAUSSIAN BEAM IN A KERR MEDIUM

A. Propagation Equations

In this section we first introduce the differential equations that describe the propagation of an astigmatic Gaussian beam through a Kerr medium; then we derive and comment on a linearized set of equations that are valid for low-power beams. In this study we consider Gaussian beams with simple astigmatism,[30] so the axis of the elliptical light spot does not rotate during propagation. We denote by z the propagation axis and by x and y two orthogonal transverse axes. The spot sizes (half-width $1/e$ of the field amplitude) are w_x and w_y, and the radii of curvature are R_x and R_y. Throughout the paper we write all the equations only for the x direction; the corresponding equations for the y direction can easily be obtained when the x and y subscripts are exchanged.

The propagation of astigmatic Gaussian beams in a Kerr medium is governed by the paraxial wave equation that, with the aberrationless approximation, leads to a set of coupled differential equations[22]:

$$\frac{\mathrm{d}^2 w_x}{\mathrm{d}z^2} = \left(\frac{\lambda}{n\pi}\right)^2 \frac{1}{{w_x}^3}\left(1 - \frac{w_x}{w_y}\, p\right),$$

$$\frac{\mathrm{d}w_x}{\mathrm{d}z} = \frac{w_x}{R_x}, \tag{1}$$

where λ is the vacuum wavelength, n is the linear refractive index, and $p = P/P_c$ is the beam power P normalized to the critical power P_c for self-trapping. With the nonlinear refractive index defined as $n_{\mathrm{NL}} = n + n_2 I$, where I is the beam intensity, various slightly different expressions of the critical power as a function of n_2 can be found in the literature.[3–6,31] One of the most accurate is derived by variational calculations and is given by $P_c = \lambda^2/(2\pi n n_2)$.[9,32]

For our purposes in this paper it is more convenient to express these equations in terms of the new variables:

$$\omega_x = {w_x}^2, \qquad \rho_x = {w_x}^2/R_x. \tag{2}$$

With this notation the propagation equations, after some manipulation, can be written as

$$\frac{\mathrm{d}\omega_x}{\mathrm{d}z} = 2\rho_x,$$

$$\frac{\mathrm{d}\rho_x}{\mathrm{d}z} = \frac{{\rho_x}^2}{\omega_x} + \left(\frac{\lambda}{n\pi}\right)^2 \frac{1}{\omega_x} - p\left(\frac{\lambda}{n\pi}\right)^2 \frac{1}{(\omega_x\omega_y)^{1/2}}. \tag{3}$$

For $p = 0$, Eqs. (3) can easily be solved to give the standard rule for the propagation of a Gaussian beam in a linear medium of refractive index n.[33] Thus we obtain

$$\omega_{Lx} = \omega_{x0}\left[\left(1 + \frac{\rho_{x0}}{\omega_{x0}}\, z\right)^2 + \left(\frac{\lambda z}{\pi n \omega_{x0}}\right)^2\right],$$

$$\rho_{Lx} = \rho_{x0}\left(1 + \frac{\rho_{x0}}{\omega_{x0}}\, z\right) + \left(\frac{\lambda}{\pi n}\right)^2 \frac{z}{\omega_{x0}}, \tag{4}$$

where the subscript L stands for linear (i.e., $p = 0$) and ω_{x0} and ρ_{x0} are the initial conditions for $z = 0$.

It is essential for the derivation presented in Subsection 2.B that for an infinitesimal propagation length $\mathrm{d}z$ Eqs. (3) give the change in spot size and radius of curvature as

$$\mathrm{d}\omega_x = 2\rho_x \mathrm{d}z,$$

$$\mathrm{d}\rho_x = \left[\frac{{\rho_x}^2}{\omega_x} + \left(\frac{\lambda}{n\pi}\right)^2 \frac{1}{\omega_x}\right]\mathrm{d}z - p\left(\frac{\lambda}{n\pi}\right)^2 \frac{1}{(\omega_x\omega_y)^{1/2}}\,\mathrm{d}z. \tag{5}$$

The Kerr effect for an infinitesimal propagation does not influence the spot sizes, which suffer the same variations as for a linear propagation, whereas the wave-front curvatures are affected by an additional nonlinear change proportional to the beam power. Therefore, a small slice of a Kerr medium, in agreement with the physical intuition, behaves as a thin nonlinear lens, with the dioptric power for the x direction, ϕ_x, given by

$$\phi_x = p\left(\frac{\lambda}{n\pi}\right)^2 \left(\frac{\omega_x}{\omega_y}\right)^{1/2} \frac{1}{{\omega_x}^2}\,\mathrm{d}z. \tag{6}$$

Note that the dioptric power expressed by Eq. (6) should be calculated with the spot sizes at $p = 0$ to yield a first-order approximation.

Since we are interested in the propagation of a low-power beam, we can linearize the equation by approximating ω_x and ρ_x as

$$\omega_x(p) \cong \omega_{Lx} + p\omega_{Kx},$$

$$\rho_x(p) \cong \rho_{Lx} + p\rho_{Kx}. \tag{7}$$

Inserting the above expressions into Eqs. (3) and neglecting the terms in p with exponents larger than 1, we obtain the following linear differential equations for ω_{Kx} and ρ_{Kx}:

$$\frac{\mathrm{d}\omega_{Kx}}{\mathrm{d}z} = 2\rho_{Kx},$$

$$\omega_{Lx}\frac{\mathrm{d}\rho_{Kx}}{\mathrm{d}z} = 2\rho_{Lx}\rho_{Kx} - \frac{\mathrm{d}\rho_{Lx}}{\mathrm{d}z}\,\omega_{Kx} - \left(\frac{\lambda}{n\pi}\right)^2 \left(\frac{\omega_{Lx}}{\omega_{Ly}}\right)^{1/2}. \tag{8}$$

According to Eqs. (7) the above equations must be solved with the initial conditions (for $z = 0$) $\omega_{Kx} = 0$ and $\rho_{Kx} = 0$.

B. Solution of the Propagation Equations

Equations (8) are a set of linear equations for ω_{Kx}, ω_{Ky}, ρ_{Kx}, and ρ_{Ky} with driving terms. Instead of applying the general rules for the solution of simultaneous linear differential equations, we present a simpler derivation based on physical reasoning. The problem is the calculation of the beam parameters inside the Kerr medium in a generic position, z, along the propagation direction once the parameters at the input plane ($z = 0$) are known. Consider, as illustrated in Fig. 1, a thin slice of Kerr medium of thickness $\mathrm{d}\zeta$ at a distance ζ from the input plane: this piece of material induces a nonlinear variation in the beam parameters that can be linearly propagated to the output plane, since the Kerr effect in the remaining part of the material produces modifications that are of the second order in the power p and can thus be neglected. For the same reason the effect of this thin slice on the nonlinear beam-parameter modifications

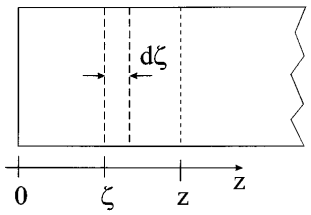

Fig. 1. Coordinate system used for study of nonlinear propagation in a Kerr medium.

induced by the preceding propagation can be neglected. According to Eq. (6) the nonlinear effect of the thin slice is that of a thin lens in the plane at ζ, which results in a change $d\omega_{Kx}$ of the spot size at the output plane z. To the first order in p we can calculate $d\omega_{Kx}$ as

$$d\omega_{Kx}(z) = \left(\frac{d\omega_x(z)}{d\phi_x}\right)_{\phi_x=0}\left(\frac{d\phi_x}{dp}\right)_{p=0}, \tag{9}$$

where, according to the *ABCD* law[33] for propagation through a thin lens of dioptric power ϕ_x and a distance $z - \zeta$, $\omega_x(z)$ is given by

$$\omega_x(z) = \omega_{Lx}(\zeta)\left\{\left[1 - (z-\zeta)\phi_x + (z-\zeta)\frac{\rho_{Lx}}{\omega_{Lx}}\right]^2 + \left[\frac{\lambda(z-\zeta)}{\pi n \omega_{Lx}}\right]^2\right\}. \tag{10}$$

With Eqs. (10) and (6), Eq. (9) simplifies to

$$d\omega_{Kx}(z) = -2\left(\frac{\lambda}{\pi n}\right)^2\left(\frac{\omega_{Lx}}{\omega_{Ly}}\right)^{1/2}\left[1 + \frac{z-\zeta}{\omega_{Lx}(\zeta)}\rho_{Lx}(\zeta)\right] \times \frac{z-\zeta}{\omega_{Lx}(\zeta)}\,d\zeta. \tag{11}$$

Taking into account Eq. (3), in conclusion, we can write Eq. (11) as

$$d\omega_{Kx}(z) = \left(\frac{\lambda}{\pi n}\right)^2\left[\frac{\omega_{Lx}(\zeta)}{\omega_{Ly}(\zeta)}\right]^{1/2}\frac{d}{d\zeta}\left[\frac{(z-\zeta)^2}{\omega_{Lx}(\zeta)}\right]d\zeta. \tag{12}$$

We can obtain the total change in the spot size at the output plane by adding all the contributions from the slices in which the Kerr medium is split; thus

$$\omega_{Kx}(z) = \left(\frac{\lambda}{\pi n}\right)^2\int_0^z\left[\frac{\omega_{Lx}(\zeta)}{\omega_{Ly}(\zeta)}\right]^{1/2}\frac{d}{d\zeta}\left[\frac{(z-\zeta)^2}{\omega_{Lx}(\zeta)}\right]d\zeta. \tag{13}$$

According to Eqs. (8) the curvature is given by the derivative of the spot size with respect to the propagation coordinate, which can be easily calculated from Eq. (13) to give

$$\rho_{Kx}(z) = \left(\frac{\lambda}{\pi n}\right)^2\int_0^z\left[\frac{\omega_{Lx}(\zeta)}{\omega_{Ly}(\zeta)}\right]^{1/2}\frac{d}{d\zeta}\left(\frac{z-\zeta}{\omega_{Lx}(\zeta)}\right)d\zeta. \tag{14}$$

The expressions for the nonlinear spot size and curvature variations given by Eqs. (13) and (14) might appear to be rather crude approximations; however, it can be confirmed by direct substitution that they are indeed the exact solutions of Eqs. (8); therefore they are the exact first-order solutions. In particular, for a cylindrically symmetric beam $\omega_x = \omega_y$, and the integral in Eq. (13) can immediately be calculated, so we obtain

$$\omega_{Kx}(z) = \omega_{Ky}(z) = -\left(\frac{\lambda}{\pi n}\right)^2\frac{z^2}{\omega_{Lx}(0)}. \tag{15}$$

This equation agrees with the results reported in Refs. 7–9 for cylindrically symmetric beams. Its validity is not limited to the first order in p, but it is the exact solution of Eqs. (3) within the aberrationless approximation.

C. Comparison with Numerical Results

In this subsection, to assess the validity of the method described above, we compare its results with the numerical solution of the nonlinear simultaneous differential equations (1), obtained by an high-accuracy fourth-order Runge–Kutta method implemented with the high-level MATLAB language (version 4.0, MathWorks Inc., Natik, Massachusetts, 1993). We consider a configuration simi-

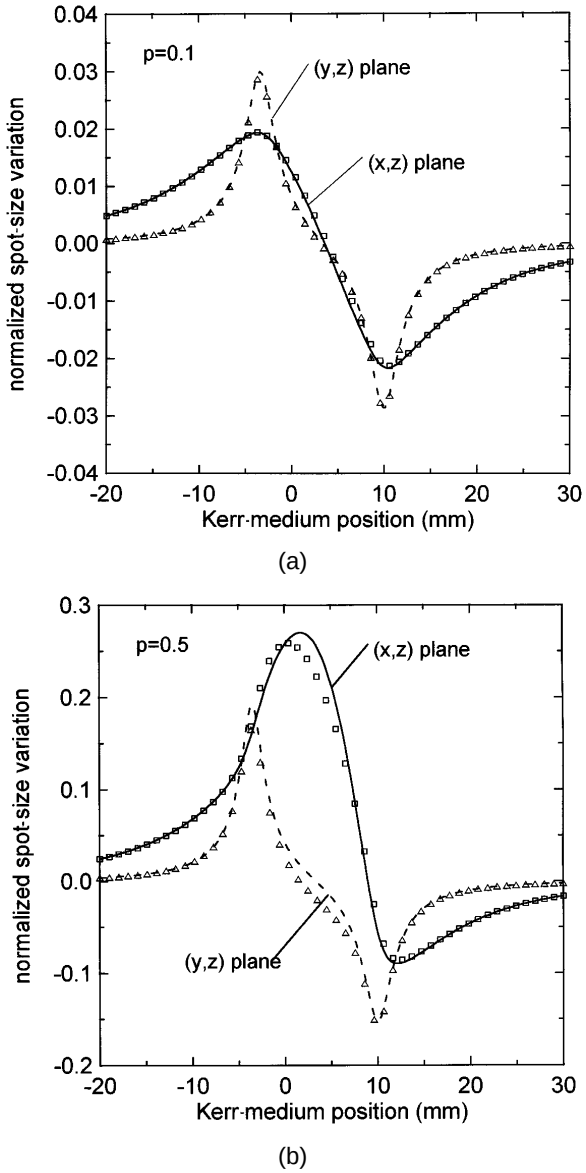

Fig. 2. (a) *Z*-scan experiment simulation for an astigmatic Gaussian beam with wavelength $\lambda = 0.8\ \mu$m, normalized power $p = 0.1$, and coincident waists with spot sizes $w_{x0} = 60\ \mu$m and $w_{y0} = 20\ \mu$m, through a 20-mm-long Kerr medium with $n = 1.5$. The Kerr medium position is the distance between its center and the beam waist without the Kerr medium. Spot-size variations on the output plane (normalized to the linear spot size) are observed in the beam far field at a distance of 300 mm from the waist. Dots are obtained with the numerical solution of Eqs. (1). (b) Same as in (a), but $p = 0.5$.

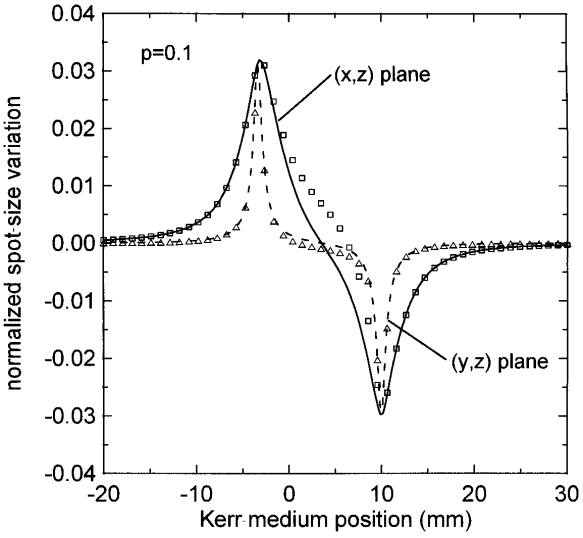

(a)

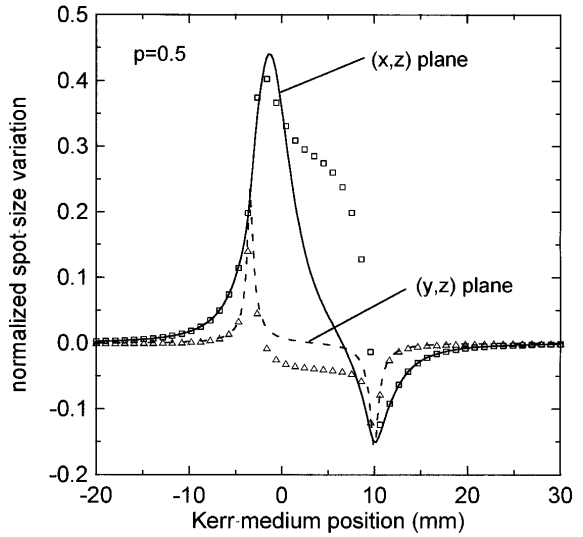

(b)

Fig. 3. (a) Same as in Fig. 2(a), with $w_{x0} = 30\ \mu$m, $w_{y0} = 10\ \mu$m, and $p = 0.1$. (b) Same as in (a), but $p = 0.5$.

lar to that of a classical Z-scan experiment,[34] in which a Kerr medium is moved around the waist of an astigmatic Gaussian beam and the beam spot-size variations in the far field are observed. As a first example we used a Kerr medium with length $l = 20$ mm, refractive index $n = 1.5$, and an astigmatic Gaussian beam with the same position of the beam waists in the (x, z) and (y, z) planes, with spot sizes at the beam waists $w_{x0} = 60\ \mu$m and $w_{y0} = 20\ \mu$m. Figure 2(a) shows the spot-size variations in the (x, z) and the (y, z) planes, obtained with Eqs. (13) and (14) used for $p = 0.1$, as a function of the distance between the center of the Kerr medium and the position of the beam waist without the Kerr medium[34]; Fig. 2(b) shows the results of the same calculations repeated for $p = 0.5$. The same figures also show the points obtained with the numerical solution of Eqs. (1). In this case there is a good agreement between the analytical and the numerical results even for high values of the normalized power. Figures 3(a) and 3(b) show the results for a more tightly focused beam, with $w_{x0} = 30\ \mu$m and $w_{y0} = 10\ \mu$m. These computations emphasize that, under focusing conditions for which the confocal parameter[35] of the beam in one direction becomes much smaller than (approximately one tenth of) the Kerr medium length, the first-order analytical approximation does not correctly describe the beam propagation in the Kerr medium; this is, however, a quite unusual focusing condition. The disagreement becomes more pronounced for higher values of the normalized power, of the order of $p = 0.4–0.5$.

Note that, owing to the coupled nature of Eqs. (1), the results obtained with astigmatic and cylindrically symmetric beam treatments can be substantially different. As an example, in Fig. 4 we compare the previous results with those obtained, for the (x, z) and (y, z) planes, respectively, by use of the propagation equations for a cylindrically symmetric beam. In this case the predictions of the cylindrically symmetric beam treatment are not even qualitatively correct.

3. KERR-LENS SENSITIVITY OF ASTIGMATIC RESONATORS

A. Analytical Derivation

Our purpose in this section is to calculate, according to the previously derived formalism, the self-consistent Gaussian beam in an astigmatic resonator containing a Kerr medium. We consider only resonators containing orthogonal astigmatic optical systems,[30,36] which implies that the propagation of the beam parameters in the x and the y transverse directions outside the Kerr medium are independent. This is by far the most common practical situation in resonators used for KLM. The most important resonator parameter that we need for study of mode locking is the derivative of the beam spot size with respect to the beam power, calculated for vanishing power at the plane inside the resonator where the aperture is placed[9,14,18,29,37]:

$$\delta = \left(\frac{1}{2\omega} \frac{\mathrm{d}\omega}{\mathrm{d}p} \right)_{p=0} . \tag{16}$$

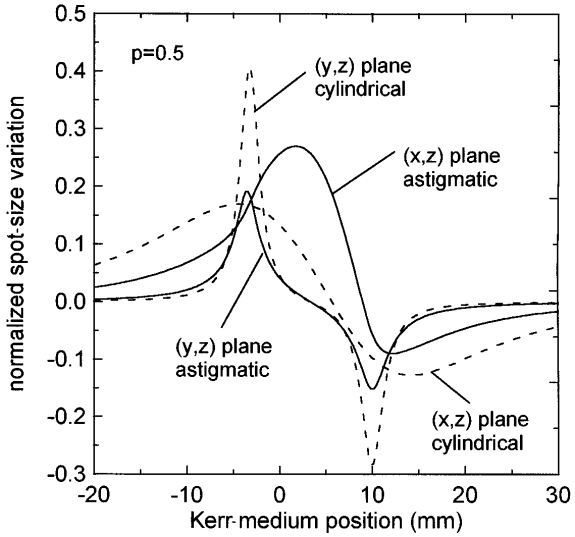

Fig. 4. Comparison of the analytical astigmatic beam results (solid curves) with those obtained by use of, for the (x, z) and the (y, z) planes, cylindrically symmetric beam propagation (dashed curves). Parameters for the calculations are as in Fig. 2(b).

Here we refer to this parameter as the Kerr-lens sensitivity, whereas in previous publications[9,18,29,37] we called it the small-signal relative spot-size variation. Since the variations of the cavity losses with power are, to the first order, proportional to δ,[14,18,29] KLM is possible only if a suitable aperture is placed in a position corresponding to negative values of δ, and self-starting KLM becomes possible if the magnitude of δ is large enough.[26–29]

Here we present a simple procedure for the calculation of δ, based on the same physical reasoning that was used to obtain the solution of the propagation equations presented in Section 2: first we calculate the spot-size variation on one of the end mirrors that is due to a thin slice of Kerr medium, neglecting the self-focusing effect in the remaining part; then we integrate over the whole length of the material to get the total variation. The most general configuration of a resonator containing a Kerr medium is shown in Fig. 5: it includes two arbitrary orthogonal astigmatic optical systems and a Kerr medium of length l and refractive index n. Possible Brewster interfaces of the Kerr medium are thought to be included in the optical systems and can be described by suitable *ABCD* ray matrices.[38] The cavity end mirrors are assumed to be flat because the effect of their curvature can also be included in the matrices representing the optical systems. Since a slice of a Kerr medium of thickness $\mathrm{d}\zeta$ is equivalent to a thin lens, the square of the spot size ω_1 on the end cavity mirror M_1 can be calculated with the standard *ABCD* law once this thin lens is included in the resonator matrix. The contribution to the Kerr-lens sensitivity on mirror M_1 that is due to this lens can therefore be expressed as

$$\mathrm{d}\delta_{1x} = \left(\frac{1}{2\omega_{1x}}\,\frac{\mathrm{d}\omega_{1x}}{\mathrm{d}\phi_x}\right)_{\phi_x=0}\left(\frac{\mathrm{d}\phi_x}{\mathrm{d}p}\right)_{p=0}, \tag{17}$$

where ϕ_x is the dioptric power of the thin slice of the Kerr medium as given by Eq. (6). The beam parameters used in Eq. (17) can be expressed as a function of the elements of the ray matrices of the optical systems contained inside the resonator by use of the standard *ABCD* laws, and the derivative can thus be calculated. The details of the derivation are presented in Appendix A. Integration over the length of the whole Kerr medium provides the following final formula:

$$\delta_{1x} = -\frac{1}{n}\left(\frac{1-S_y{}^2}{1-S_x{}^2}\right)^{1/4}\int_0^l \left|\frac{\tilde{B}_x}{\tilde{B}_y}\right|^{1/2} \times \frac{B_{2x}D_{2x}S_x + B_{1x}D_{1x}}{\tilde{B}_x{}^2}\,\mathrm{d}\zeta\,. \tag{18}$$

The symbols used in the above equation, according to Fig. 5, are defined as follows: ζ is the longitudinal coordinate in the Kerr medium ($0 \le \zeta \le l$); $\tilde{B}_x$ and $\tilde{B}_y$ are the (1,2) elements of the round-trip matrices around the resonator from the position ζ; B_{1x}, D_{1x} and B_{2x}, D_{2x} are the matrix elements relevant for the propagation from the position ζ to mirrors M_1 and M_2, respectively; and S_x and S_y are the stability factors for the x and the y directions, defined as half the trace of the round-trip matrices. With the symbols defined in Fig. 5, S_x can be written as

$$S_x = \frac{\tilde{A}_x + \tilde{D}_x}{2} = A_xD_x + B_xC_x\,, \tag{19}$$

where A_x, B_x, C_x, and D_x are the elements of the one-way matrix from M_1 to M_2. The matrix elements in Eqs. (18) and (19) must be calculated for $p = 0$ and are, in general, functions of ζ, except S_x and S_y, which are invariant.[39] Note that for a stable resonator $-1 < S_x, S_y < 1$.[39] As is shown in Appendix A, the Kerr-lens sensitivity can also be expressed in the following form, which could be useful for the numerical calculation:

$$\delta_{1x} = \frac{1}{2n}\left(\frac{1-S_y{}^2}{1-S_x{}^2}\right)^{1/4}\int_0^l \left|\frac{\tilde{B}_x}{\tilde{B}_y}\right|^{1/2}\,\frac{\mathrm{d}}{\mathrm{d}\zeta}\left(\frac{B_{2x}D_{2x}}{\tilde{B}_x}\right)\mathrm{d}\zeta\,. \tag{20}$$

The integrals in Eqs. (18) and (20) are not, in general, elementary functions but can be reduced to combinations of elliptic integrals, since the square root contains the ratio between two second-degree polynomials and the other term in the integral is a rational function of ζ; the result, however, is quite involved and is not reported here. Obviously one can obtain the Kerr-lens sensitivity for the y direction and those on mirror M_2 simply by exchanging the subscripts x with y and 1 with 2, whereas the expression for this parameter in an arbitrary plane inside the resonator is given in Appendix B.

It may be worthwhile to emphasize that Eqs. (18) and (20) are not approximate but give the actual value of δ_1 (within the aberrationless theory): to confirm this, we have also derived δ_1 by the following alternative procedure, which gives results coincident with those of Eqs. (18) and (20). The propagation rules in the Kerr medium derived in Section 2, the *ABCD* law for the propagation of the beam in the linear sections of the resonator, and the self-consistency condition after a round trip were used to construct simultaneous equations whose solution gives the mode spot size as a function of power. The derivative of the mode spot size with respect to p for $p = 0$ gives, according to Eq. (16), the Kerr-lens sensitivity. This procedure is, however, quite involved and is not reported here.

For a cylindrically symmetric resonator the parameters along the x and the y directions are identical; therefore the integral in Eq. (20) can immediately be calculated and expressed as

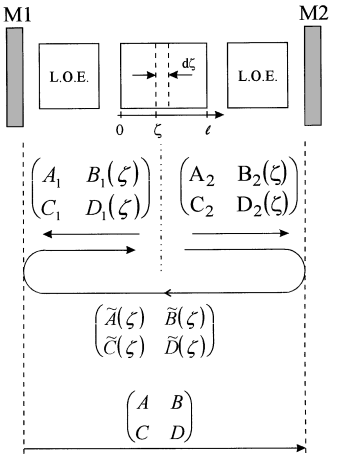

Fig. 5. General configuration of a resonator containing a Kerr medium; the arrows indicate the directions to which the matrices refer. Subscripts x and y of the matrix elements are omitted. L.O.E., linear optical elements; M1, mirror M_1; M2, mirror M_2.

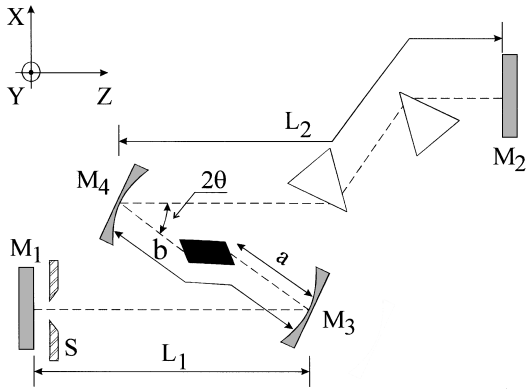

Fig. 6. Resonator configuration of a KLM laser used for both the calculations and the experiments. M_1, M_2 flat mirrors; M_3, M_4, concave folding mirrors (radius of curvature 100 mm, incidence angle $\theta = 14.8°$); S, slit; the medium is a Brewster-cut Ti:sapphire rod with $l = 20$ mm and $n = 1.76$. Folding-mirror distance b is the physical path length between the mirrors.

$$\delta_1 = \frac{1}{2n}\left[\left(\frac{B_2 D_2}{\tilde{B}}\right)_{\zeta=l} - \left(\frac{B_2 D_2}{\tilde{B}}\right)_{\zeta=0}\right], \tag{21}$$

where the subscripts x and y have been dropped as a result of symmetry. By simple but rather tedious algebraic manipulation it can be confirmed that Eq. (21) coincides with the formulas that we derived using a nonlinear *ABCD* matrix and reported in previous papers.[18,37]

B. Comparison with Numerical Results

To test the correctness of the analytical derivation, the Kerr-lens sensitivity of an astigmatic resonator was also calculated with an iterative numerical method. In this approach an astigmatic Gaussian beam was propagated back and forth through the cavity until a self-consistent solution was reached.[2,21] The beam was propagated through the linear sections of the resonator by use of the *ABCD* law and through the Kerr medium by numerical solution of the simultaneous differential equations (1) with the Runge–Kutta method for a given value of the normalized power, p. Once the self-consistent mode was found, the Kerr-lens sensitivity was obtained as

$$\delta_{1x} \approx \frac{1}{2\omega_{1Lx}} \frac{\omega_{1x} - \omega_{1Lx}}{p},$$

where ω_{1Lx} is the linear spot size on mirror M_1 and ω_{1x} the nonlinear one; obviously this is a good approximation if p is chosen small enough.

A typical resonator used for KLM lasers is shown in Fig. 6: it is a z-type four-mirror astigmatically compensated folded cavity with the active medium cut at Brewster's angle. Figure 7(a) shows, for a symmetric configuration ($L_1 = L_2 = 850$ mm) and in the tangential (x, z) plane, the analytical calculation of the Kerr-lens sensitivity on cavity end mirror M_1, obtained from Eq. (20); Fig. 7(b) shows the same for the sagittal (y, z) plane. The results of the iterative numerical calculations are also shown in Figs. 7(a) and 7(b) as points; they confirm the correctness of our analytical approach.

In previous publications[29,37] we calculated the Kerr-lens sensitivity of astigmatic resonators by splitting them into equivalent uncoupled one-dimensional resonators for the tangential and the sagittal planes and applying to each of them the cylindrically symmetric beam treatment. The results of this approximation are shown in Figs. 7(a) and 7(b) as dashed curves; it can be seen that for the tangential plane the approximation is in qualitative agreement with the more exact astigmatic treatment, whereas in the sagittal plane the results are quite different. This comparison shows that astigmatism effects must be fully taken into account in the analysis and design of KLM resonators.

4. RESONATORS FOR KERR-LENS MODE LOCKING

A. Resonator Design Tool: Kerr-Lens Sensitivity Contour Lines

Our purpose in this section is to study, with the formalism outlined above, some of the resonators most commonly

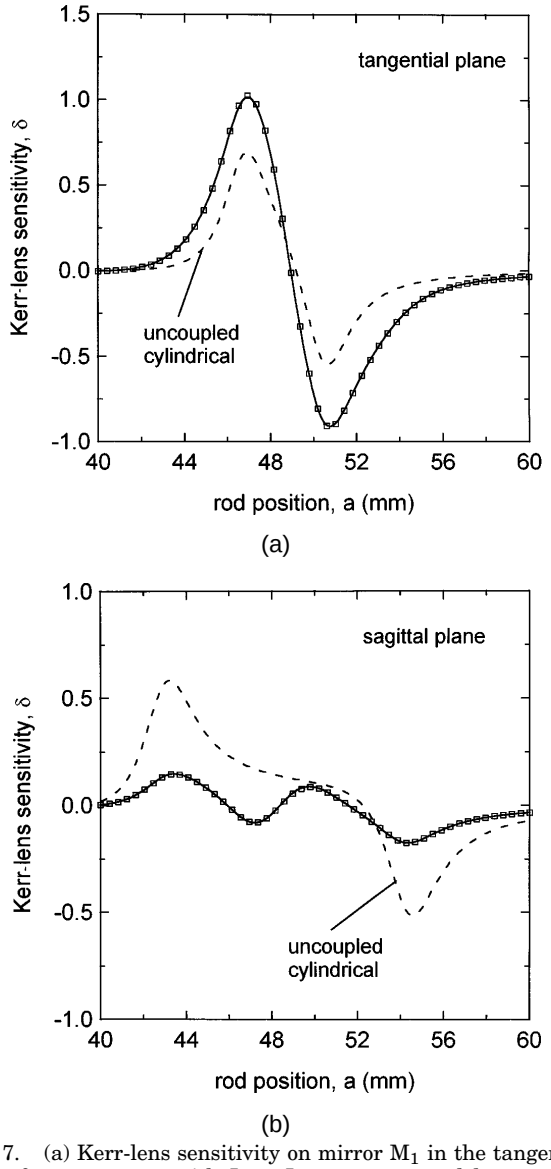

Fig. 7. (a) Kerr-lens sensitivity on mirror M_1 in the tangential plane for a resonator with $L_1 = L_2 = 850$ mm and $b = 117$ mm as a function of the rod position a. The solid curve is obtained from Eq. (20); points are the results of an iterative numerical calculation performed with $p = 0.01$; the dashed curve is obtained by application of the cylindrically symmetric beam treatment to the equivalent uncoupled one-dimensional resonator. (b) Same as in (a) but for the sagittal plane.

used for KLM lasers in order to derive design guidelines and to identify an optimized configuration.

For mode locking to be achieved, an aperture must be inserted inside the resonator in a position at which the Kerr-lens sensitivity δ is negative. The resonator parameters that most deeply influence δ are the folding-mirror distance, b, and the distance between mirror M_3 and the closer face of the rod, a. The parameter b essentially determines the optical stability, while a controls the focusing condition. As a useful design tool for KLM lasers we propose the plot of the contour lines of δ as a function of the resonator parameters a and b. These plots can be used to identify the resonator configuration that provides the strongest nonlinear mode variations and permits the widest tolerances on the positions of the components for successful KLM.

As an example, Fig. 8 shows contour lines for an asymmetric resonator ($L_1 = 500$ mm, $L_2 = 1100$ mm) in the tangential plane; this resonator presents two regions of optical stability as a function of the folding-mirror distance b.[40] Figure 9 shows the same results for the sagittal plane. It can be seen that in the tangential plane there are broader regions of negative δ than in the sagittal one. The strongest nonlinear mode variations are achieved near the resonator optical stability limits[11,13,14,17–20]; however, they are difficult to exploit experimentally, because near the stability limits the mode spot size in the active material and the output power change rapidly as the resonator parameters are slightly varied.

Figure 10 shows the contour lines for a symmetric resonator ($L_1 = L_2 = 850$ mm) in the tangential plane, and Fig. 11 those in the sagittal plane. For this cavity the two regions of optical stability are joined and result in a single stability region in terms of b. At the stability limit b_m, corresponding to the center of this wider region, the resonator can be shown to be equivalent to a confocal one, with a well-behaved transverse mode. Also for the symmetric resonator, the nonlinear mode variations are stronger in the tangential plane.

A comparison of the contour lines of δ for different resonators permits the following conclusions to be drawn: (i) The effect of astigmatic beam coupling in most resonators used in practice for KLM is to increase the Kerr lens sensitivity in the tangential plane and reduce it in the sagittal one; therefore the slit used to induce KLM should cut the beam in the tangential plane.[17] (ii) The folding-mirror angle is also an important parameter to be considered. The astigmatically compensated resonators,[41] which provide the largest overlap between the stability zone in tangential and sagittal planes, also represent the best choice for the highest Kerr-lens sensitivity. (iii) KLM can be obtained with most resonators, provided that the folding distance b and the rod position a are properly adjusted. (iv) In general, symmetric resonators present broader regions of negative Kerr-lens sensitivity, so that they allow for greater tolerances in the cavity configuration for KLM. Note that this conclusion is in contrast to the one reported in Ref. 17. In fact, in Ref. 17 the comparison between symmetric and asymmetric resonators was performed with the rod kept in a particular position inside the folding; thus the effect of the rod position was not fully analyzed. (v) In symmetric resonators it is possible to achieve large values of δ by approaching the tangential central stability limit b_{mx} without laser power degradation. Even with a short Kerr medium, as is needed for very short pulses (10–20 fs), large values of the Kerr-lens sensitivity can be obtained, provided that a

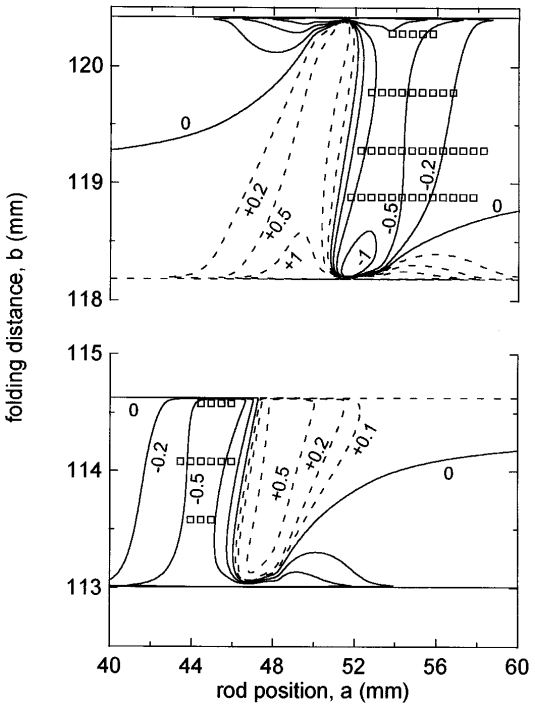

Fig. 8. Contour lines of the Kerr-lens sensitivity δ_{1x} (parameter of the curves) as a function of a and b in the tangential plane for an asymmetric resonator with $L_1 = 500$ mm and $L_2 = 1100$ mm. The squares mark the points for which KLM was experimentally achieved with a slit on mirror M_1, cutting the beam in the tangential plane. The horizontal lines are the resonator optical stability limits.

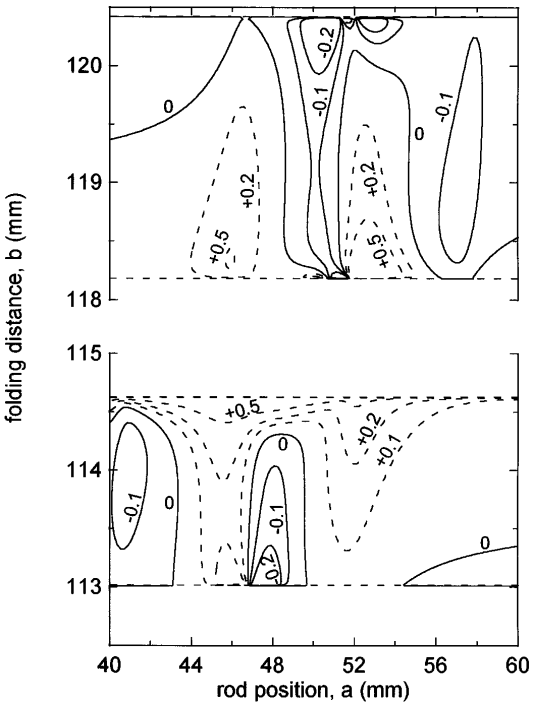

Fig. 9. Same as in Fig. 8 but in the sagittal plane.

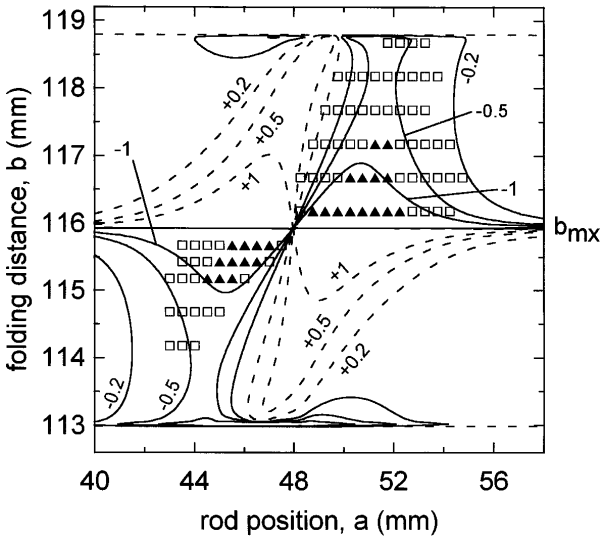

Fig. 10. Same as in Fig. 8 but for a symmetric resonator with $L_1 = L_2 = 850$ mm in the tangential plane. The squares mark the points at which KLM was initiated by our tapping on one of the end mirrors; the triangles correspond to the self-starting condition.

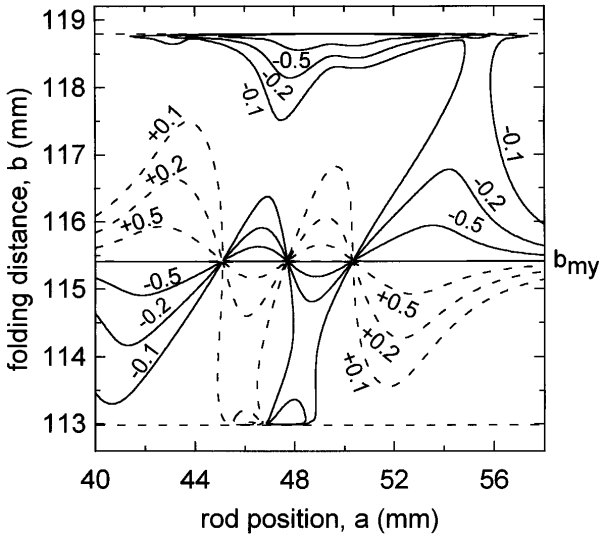

Fig. 11. Same as in Fig. 10 but in the sagittal plane.

suitable focusing condition is chosen. For these reasons we believe symmetric resonators to be more suitable than asymmetric ones for KLM with a hard aperture.

B. Experimental Results

In this section we compare the predictions of our treatment with the experimental results obtained with a KLM Ti:sapphire laser. The laser configuration used for the experiments is shown in Fig. 6: it includes a 20-mm-long Brewster-cut Ti:sapphire rod, two SF10 prisms for dispersion compensation, and a slit in front of mirror M_1 that cuts the beam in the tangential plane. The argon-ion laser pump beam was adjusted to avoid KLM by gain guiding effects. The laser rod and the folding mirrors are mounted on micrometric translators. The experimental setup and conditions are described in greater detail in Refs. 29 and 37. In particular the relative folding-mirror position was read directly on the micrometers of the translation stages, and the absolute calibration was obtained by comparison with the calculated stability limits.

First we built an asymmetric resonator with $L_1 = 500$ mm and $L_2 = 1100$ mm and systematically varied parameters a and b. For each value of a and b we tested whether KLM was possible by aligning the laser for maximum output power and progressively closing the slit; the mode-locking regime was initiated by our slightly tapping on one of the cavity end mirrors. The experimental resonator operation points for which KLM was achieved are shown in Fig. 8 as squares. The optical stability of an astigmatic resonator is determined by the overlap of the stability regions in the sagittal and the tangential planes. For this reason the limit at $b = 114.62$ mm, which corresponds to the boundary in the sagittal plane, is different from that in Ref. 37, where only the behavior of the tangential plane was considered. Note that, with respect to the data published in Ref. 37, we decreased by 0.5 mm the folding distance b of the experimental points in the lower stability zone to make them fit into the resonator optical stability region. The slight uncertainty in positioning the experimental data points could be explained by the difficulty in the calibration of the folding distance and partially by the fact that the laser can also operate with the resonator stable in one plane and unstable in the orthogonal plane as a result of gain guiding and thermal lensing in the rod.[20] It can be seen from Fig. 8 that, in agreement with the theory, KLM is possible only in the regions of the (a, b) plane with negative Kerr-lens sensitivity values.

The same series of experiments was performed with a symmetric resonator ($L_1 = L_2 = 850$ mm). The resonator operation points for which KLM was obtained by our tapping on one cavity mirror are shown in Fig. 10 as squares; in this case also there is a good agreement between the theoretical predictions and the experimental results. For this resonator, when the folding-mirror distance was adjusted in a suitable range around the central stability limit b_{mx}, the KLM regime became self-starting, so that no external perturbation was needed to initiate pulse formation. The experimental points in which self-starting KLM was achieved are shown in Fig. 10 as triangles. It can be seen that the points of self-starting operation correspond to large negative values of the Kerr-lens sensitivity δ_{1x} ($|\delta_{1x}| > 1$). The self-starting regime was stable and easily reproducible once the nonlinear loss modulation was optimized.

In conclusion, our experiments show that an astigmatic resonator design procedure based on the contour lines of the Kerr-lens sensitivity allows one to optimize KLM laser performance effectively. In particular, with symmetric resonators nonlinear loss modulations strong enough to permit self-starting of the KLM regime can be achieved.

5. CONCLUSIONS

In this paper we introduce a new analytical treatment for the propagation of an astigmatic Gaussian beam through a Kerr medium. This method is valid to the first order in the beam power and allows us to calculate in closed form the nonlinear spot-size and radius-of-curvature variations of the beam. This method has been applied to calculate analytically the power-dependent self-consistent Gauss-

ian mode for an astigmatic resonator with a Kerr medium. The nonlinear mode spot-size variation in astigmatic resonators, described by the Kerr-lens sensitivity δ, can thus be directly calculated, avoiding time-consuming iterative numerical simulations. These calculations are important for the design of KLM lasers, which often have astigmatic resonators because of the presence of a Brewster-cut Kerr medium and tilted folding mirrors. Astigmatism often produces sizable effects, therefore making the predictions of the cylindrically symmetric beam treatment inaccurate. We have proposed, as a powerful design tool for KLM lasers, the plot of the contour lines of δ as a function of the most critical resonator parameters; this plot allows one to identify the resonator configuration most suitable for KLM.

Our theoretical analysis is backed up by the experimental results obtained with a femtosecond KLM Ti:sapphire laser. The experiments confirmed that it is possible to achieve KLM by placement of a slit in a given plane inside the resonator only if the Kerr-lens sensitivity δ on that plane is negative. In particular, symmetric resonators, if suitably optimized, allow one to obtain large nonlinear spot-size variations, which result in self-starting KLM.

APPENDIX A: DERIVATION OF EQS. (18) AND (20)

As is illustrated in Fig. 5, we denote by

$$\begin{bmatrix} A_{jx} & B_{jx} \\ C_{jx} & D_{jx} \end{bmatrix},$$

where $j = 1, 2$ and $i = x, y$, the matrix from the plane ζ inside the Kerr medium to mirror M_j and by

$$\begin{bmatrix} A_x(\phi_x) & B_x(\phi_x) \\ C_x(\phi_x) & D_x(\phi_x) \end{bmatrix}$$

the one-way matrix from M_1 to M_2, including the thin lens of dioptric power ϕ_x placed in the plane ζ. By simple matrix multiplication we obtain

$$\begin{bmatrix} A_x(\phi_x) & B_x(\phi_x) \\ C_x(\phi_x) & D_x(\phi_x) \end{bmatrix} = \begin{bmatrix} A_x - D_{1x}B_{2x}\phi_x/n & B_x - B_{1x}B_{2x}\phi_x/n \\ C_x - D_{1x}D_{2x}\phi_x/n & D_x - B_{1x}D_{2x}\phi_x/n \end{bmatrix}, \quad \text{(A1)}$$

where A_x, B_x, C_x, and D_x are the matrix elements for $\phi_x = 0$. The spot size on mirror M_1 is given by[42]

$$\omega_{1x}{}^2 = -\left(\frac{\lambda}{\pi}\right)^2 \frac{B_x(\phi_x)D_x(\phi_x)}{A_x(\phi_x)C_x(\phi_x)}. \quad \text{(A2)}$$

After calculating the derivative with respect to ϕ_x for $\phi_x = 0$, simple algebraic simplications provide

$$\left(\frac{1}{2\omega_{1x}}\frac{d\omega_{1x}}{d\phi_x}\right) = \frac{1}{n(S_x{}^2 - 1)}(B_{2x}D_{2x}S_x + B_{1x}D_{1x}), \quad \text{(A3)}$$

where $S_x = A_xD_x + B_xC_x$. According to the *ABCD* law, the spot size $\omega_{Lx}(\zeta)$ in the plane ζ is given by

$$\left(\frac{\lambda}{\pi n \omega_{Lx}}\right)^2 = \frac{1 - S_x{}^2}{\tilde{B}_x{}^2}. \quad \text{(A4)}$$

Inserting Eqs. (A3), (A4), and (6) into Eq. (17) yields

$$d\delta_{1x} = -\frac{1}{n}\left(\frac{1 - S_y{}^2}{1 - S_x{}^2}\right)^{1/4}\left|\frac{\tilde{B}_x}{\tilde{B}_y}\right|^{1/2}\frac{B_{2x}D_{2x}S_x + B_{1x}D_{1x}}{\tilde{B}_x{}^2}\,d\zeta. \quad \text{(A5)}$$

Finally the integration of Eq. (A5) over the whole length of the Kerr medium results in Eq. (18).

To verify Eq. (20) we calculate the derivative contained in that integral. After expressing the matrices in the plane $z = \zeta$ as a function of those at the plane $z = 0$, the following two derivatives can easily be calculated:

$$\frac{d\tilde{B}_x}{d\zeta} = \tilde{D}_x - \tilde{A}_x, \quad \text{(A6)}$$

$$\frac{dB_{2x}D_{2x}}{d\zeta} = -(A_{2x}D_{2x} + B_{2x}C_{2x}). \quad \text{(A7)}$$

Consequently

$$\frac{d}{d\zeta}\left(\frac{B_{2x}D_{2x}}{\tilde{B}_x}\right) = -\frac{(A_{2x}D_{2x} + B_{2x}C_{2x})\tilde{B}_x + B_{2x}D_{2x}(\tilde{D}_x - \tilde{A}_x)}{\tilde{B}_x{}^2} = -2\frac{B_{2x}D_{2x}S_x + B_{1x}D_{1x}}{\tilde{B}_x{}^2}, \quad \text{(A8)}$$

where we obtain the second equality by taking into account the rule of ray-matrix composition. The above equation demonstrates the equality between Eqs. (18) and (20).

APPENDIX B: CALCULATION OF THE KERR-LENS SENSITIVITY IN A PLANE INSIDE THE RESONATOR

With reference to Fig. 5, let us consider an arbitrary plane inside the resonator to the left side of the Kerr medium, and let

$$\begin{bmatrix} A_x & B_x \\ C_x & D_x \end{bmatrix}$$

be the matrix relative to the propagation from mirror M_1 to that plane. With $\omega_x - w_x{}^2$ defined as the square of the spot size, w_x, in that plane, it follows from straightforward matrix calculations that

$$\omega_x = \omega_{1x}\left[A_x{}^2 + \left(\frac{\lambda B_x}{\pi\omega_1}\right)^2\right]. \quad \text{(B1)}$$

The Kerr-lens sensitivity δ_x in the plane under consideration can be calculated as follows:

$$\delta_x = \left(\frac{1}{2\omega_x}\frac{d\omega_x}{dp}\right)_{p=0} = \left(\frac{\omega_{1x}}{\omega_x}\frac{d\omega_x}{d\omega_{1x}}\right)_{p=0}\delta_{1x} = \frac{A_x{}^2 - (\lambda B_x/\pi\omega_{1Lx})^2}{A_x{}^2 + (\lambda B_x/\pi\omega_{1Lx})^2}\,\delta_{1x}, \quad \text{(B2)}$$

where ω_{1Lx} is the linear spot size on mirror M_1. Obviously the same procedure can be followed for the calculation of the Kerr-lens sensitivity for the y direction or in a plane to the right-hand side of the Kerr medium (starting the calculations from mirror M_2). It can immediately be shown from Eq. (B2) that $|\delta_x| \le |\delta_{1x}|$, so the maximum

values of $|\delta_x|$ are obtained on the cavity end mirrors, on their image planes ($B_x = 0$, $\delta_x = \delta_{1x}$), or on their Fourier planes ($A_x = 0$, $\delta_x = -\delta_{1x}$).[36]

ACKNOWLEDGMENTS

The authors thank Igor Piffari for his help with the experiments.

REFERENCES

1. D. E. Spence, P. N. Kean, and W. Sibbett, "60-fsec pulse generation from a self-mode-locked Ti:sapphire laser," Opt. Lett. **16,** 42–44 (1991).
2. F. Salin, J. Squier, and M. Piché, "Mode locking of Ti:Al_2O_3 lasers and self-focusing: a Gaussian approximation," Opt. Lett. **16,** 1674–1676 (1991).
3. S. A. Akhmanov, R. V. Khokhlov, and A. P. Sukhorukov, "Self-focusing, self-defocusing and self-modulation of laser beams," in *Laser Handbook*, F. T. Arecchi and E. O. Schulz-Dubois, eds. (North-Holland, Amsterdam, 1972), pp. 1151–1228.
4. J. H. Marburger, "Self-focusing: theory," in *Progress in Quantum Electronics*, J. H. Sanders and S. Stenholm, eds. (Pergamon, Oxford, 1977), Vol. 4, pp. 35–110.
5. Y. R. Shen, "Self-focusing: experimental," in *Progress in Quantum Electronics*, J. H. Sanders and S. Stenholm, eds. (Pergamon, Oxford, 1977), Vol. 4, pp. 1–34.
6. Y. R. Shen, *The Principles of Nonlinear Optics* (Wiley, New York, 1984), Chap. 17.
7. P. A. Belanger and C. Pare, "Self-focusing of Gaussian beams: an alternate derivation," Appl. Opt. **22,** 1293–1295 (1983).
8. D. Huang, M. Ulman, L. H. Acioli, H. A. Haus, and J. G. Fujimoto, "Self-focusing-induced saturable absorber loss for laser mode locking," Opt. Lett. **17,** 511–513 (1992).
9. V. Magni, G. Cerullo, and S. De Silvestri, "*ABCD* matrix analysis of propagation of Gaussian beams through Kerr media," Opt. Commun. **96,** 348–355 (1993).
10. M. Piché, "Beam reshaping and self-mode-locking in nonlinear laser resonators," Opt. Commun. **86,** 156–160 (1991).
11. D. Georgiev, J. Hermann, and U. Stamm, "Cavity design for optimum nonlinear absorption in Kerr-lens mode-locked solid-state lasers," Opt. Commun. **92,** 368–375 (1992).
12. O. E. Martinez and J. L. A. Chilla, "Self-mode-locking of Ti:sapphire lasers: a matrix formalism," Opt. Lett. **17,** 1210–1212 (1992).
13. T. Brabec, Ch. Spielmann, P. F. Curley, and F. Krausz, "Kerr-lens mode locking," Opt. Lett. **17,** 1292–1294 (1992).
14. H. A. Haus, J. G. Fujimoto, and E. P. Ippen, "Analytic theory of additive pulse and Kerr lens mode locking," IEEE J. Quantum Electron. **28,** 2086–2096 (1992).
15. G. W. Pearson, C. Radzewicz, and J. S. Krasinski, "Analysis of self-focusing mode-locked lasers with additional highly nonlinear self-focusing elements," Opt. Commun. **94,** 221–226 (1992).
16. M. Piché and F. Salin, "Self-mode locking of solid-state lasers without apertures," Opt. Lett. **18,** 1041–1043 (1993).
17. T. Brabec, P. F. Curley, Ch. Spielmann, E. Witner, and A. J. Schmidt, "Hard-aperture Kerr-lens mode locking," J. Opt. Soc. Am. B **10,** 1029–1034 (1993).
18. V. Magni, G. Cerullo, and S. De Silvestri, "Closed form Gaussian beam analysis of resonators containing a Kerr medium for femtosecond lasers," Opt. Commun. **101,** 365–370 (1993).
19. K. H. Lin and W. F. Hsieh, "Analytical design of symmetrical Kerr-lens mode-locking laser cavities," J. Opt. Soc. Am. B **11,** 737–741 (1994).
20. J. Herrmann, "Theory of Kerr-lens mode locking: role of self-focusing and radially varying gain," J. Opt. Soc. Am. B **11,** 498–512 (1994).
21. R. E. Bridges, R. W. Boyd, and G. P. Agrawal, "Effect of beam ellipticity on self-mode locking in lasers," Opt. Lett. **18,** 2026–2028 (1993).
22. C. R. Giuliano, J. H. Marburger, and A. Yariv, "Enhancement of self-focusing threshold in sapphire with elliptical beams," Appl. Phys. Lett. **21,** 58–60 (1972).
23. A. M. Goncharenko, Yu. A. Logvin, A. M. Sanson, P. S. Shapovalov, and S. I. Turovets, "Ermakov Hamiltonian systems in nonlinear optics of elliptic Gaussian beams," Phys. Lett. A **160,** 138–142 (1991).
24. A. M. Goncharenko, Yu. A. Logvin, A. M. Sanson, and P. S. Shapovalov, "Rotating elliptical Gaussian beams in nonlinear media," Opt. Commun. **81,** 225–230 (1991).
25. F. Cornolti, M. Lucchesi, and B. Zambon, "Elliptic Gaussian beam self-focusing in nonlinear media," Opt. Commun. **75,** 129–135 (1990).
26. F. Krausz, T. Brabec, and C. Spielmann, "Self-starting passive mode locking," Opt. Lett. **16,** 235–237 (1991).
27. J. Herrmann, "Starting dynamic, self-starting condition and mode-locking threshold in passive, coupled cavity or Kerr-lens mode-locked solid-state lasers," Opt. Commun. **98,** 111–116 (1993).
28. Ming Lai, "Self-starting, self-mode-locked Ti:sapphire laser," Opt. Lett. **19,** 722–724 (1994).
29. G. Cerullo, S. De Silvestri, and V. Magni, "Self-starting Kerr-lens mode-locking of a Ti:sapphire laser," Opt. Lett. **19,** 1040–1042 (1994).
30. J. A. Arnaud and H. Kogelnik, "Gaussian light beams with general astigmatism," Appl. Opt. **8,** 1687–1693 (1969).
31. M. Sheik-bahae, A. A. Said, D. J. Hagan, M. J. Soileau, and E. W. Van Stryland, "Nonlinear refraction and optical limiting in thick media," Opt. Eng. **30,** 1228–1235 (1991).
32. M. Desaix, D. Anderson, and M. Lisak, "Variational approach to collapse of optical pulses," J. Opt. Soc. Am. B **8,** 2082–2086 (1991).
33. H. Kogelnik, "Imaging of optical modes—resonators with internal lenses," Bell Syst. Tech. J. **44,** 455–494 (1965).
34. M. Sheik-Bahae, A. A. Said, and E. W. Van Stryland, "High-sensitivity, single-beam n_2 measurements," Opt. Lett. **14,** 955–957 (1989).
35. A. E. Siegman, *Lasers* (Oxford U. Press, Oxford, 1986), Chap. 17.
36. Ref. 35, Chap. 15.
37. G. Cerullo, S. De Silvestri, V. Magni, and L. Pallaro, "Resonators for Kerr-lens mode-locked femtosecond Ti:sapphire lasers," Opt. Lett. **19,** 807–809 (1994).
38. J. P. Taché, "Ray matrices for tilted interfaces in laser resonators," Appl. Opt. **26,** 427–429 (1987).
39. Ref. 35, Chap. 21.
40. V. Magni, S. De Silvestri, and A. Cybo-Ottone, "On the stability, mode properties, and misalignment sensitivity of femtosecond dye laser resonators," Opt. Commun. **82,** 137–144 (1991).
41. H. W. Kogelnik, E. P. Ippen, A. Dienes, and C. V. Shank, "Astigmatically compensated cavities for cw dye laser," IEEE J. Quantum Electron. **QE-8,** 373–379 (1972).
42. P. Baues, "Huygens' principle in inhomogeneous, isotropic media and a general integral equation applicable to optical resonators," Opto-Electronics **1,** 37–44 (1969).